PERGAMON

International Journal of Heat and Mass Transfer 43 (2000) 1067–1078

International Journal of HEAT and MASS TRANSFER

www.elsevier.com/locate/ijhmt

Combined laminar forced convection and thermal radiation in a helical pipe

B. Zheng, C.X. Lin, M.A. Ebadian*

Hemispheric Center for Environmental Technology, Florida International University, Miami, FL 33174, USA

Received 26 February 1999; received in revised form 16 June 1999

Abstract

The interaction phenomena between laminar forced convection and thermal radiation in a participating medium inside a helical pipe were studied numerically. The P-1 radiation model was applied to the combined convection–radiation simulations. The three-dimensional governing equations for laminar flow and heat transfer were solved with a control-volume finite difference method (CVFDM) with second-order accuracy, and the O-type structure grid was adopted in this study. The effects of thermal radiation on the convective flow and heat transfer were measured by comparing the numerical results with and without thermal radiation. The comparison showed that under the conditions examined in this paper, although the thermal radiation had no significant influence for flow and temperature fields, especially in a fully developed region, it substantially enhanced the total heat transfer in the helical pipe.

Keywords: Forced convection; Thermal radiation; Curved pipe; Laminar flow

1. Introduction

Flow and heat transfer in helical pipes with a constant circular or rectangular cross-section has been a topic of important fundamental and engineering interests during the past decades. Berger et al. [1] and Shah and Joshi [2] have given extensive reviews of fluid flow and heat transfer in helical pipes. To the authors knowledge, most of the previous studies on the convective heat transfer in helical pipes have been conducted without taking thermal radiation into account. Recent studies include those conducted by Goering et al. [3], Lin et al. [4], Bolinder and Sunden [5], Sillekens [6], Yang et al. [7], Chung and Hyun [8], Yang and Chang [9], Rao [10], Liu and Masliyah [11], Su and Friedrich [12], Eason et al. [13], Joye et al. [14], Acharya et al. [15], and Vilemas et al. [16]. However, in some engineering applications — such as nuclear reactor safety, combustion systems, solar collectors, heat exchangers, and propeller systems — the thermal radiation in fluid flowing in helical pipes is usually a significant factor that interferes with the system design and operation. This especially occurs when high temperature and a radiation participating medium are involved in the helical pipes. A study of the combined heat transfer by thermal radiation and convection in helical pipes would be valuable for understanding the physics and application of heat transfer in helical pipes. Numerical simulation is an efficient approach to investigate this problem because of some limitations in radiation experimentation.

* Corresponding author. Tel.: +1-305-348-3585; fax: +1-305-348-4176.

E-mail address: ebadian@eng.fiu.edu (M.A. Ebadian).

0017-9310/00/$ - see front matter
PII: S0017-9310(99)00214-8

Nomenclature

a radius of the helical pipe, m
A area, m^2
C_p specific heat, kJ/(kg K)
d_h hydraulic diameter of the helical pipe ($=2a$), m
f_θ local friction factor on the circumference of a pipe ($\tau_w/\frac{1}{2}\rho_\infty U_0^2$)
f_m integral average friction factor on one cross-section ($\frac{1}{2\pi}\int_0^{2\pi} f_\theta \, d\theta$)
G incident radiation, W/m
Gr Grasholf number
H pitch, m
I radiation intensity, W/cm^2 ster
k thermal conductivity, W/(m K)
n coordinate direction perpendicular to a surface
Nu_θ local Nusselt number on the circumference of a pipe $\frac{q_w d_h}{k(T_w-T_b)}$
Nu_m integral average Nusselt number on one cross-section ($\frac{1}{2\pi}\int_0^{2\pi} Nu_\theta \, d\theta$)
p pressure, N/m^2
q heat flux, W m^{-2}
Pr Prandtl number
R_c radius of the coil, m
Re Reynolds number ($=\rho U_0 d_h/\mu$)
T temperature, K
T_b fluid bulk temperature on one cross-section ($\frac{1}{\bar{u}_s A}\int_0^A u_s T \, dA$), K
U_0 inlet velocity, m/s
u_i velocity component in i-direction ($i = 1, 2, 3$), m/s
u_s axial velocity component, m/s
U_s nondimensional axial velocity (u_s/U_0)
U_{2nd} nondimensional secondary velocity
x spatial position, m
x_i master Cartesian coordinate in i-direction ($i = 1, 2, 3$), m

Greek symbols
α angle, degree
δ curvature ratio (a/R_c)
δ_{ij} Dirac delta function
ΔT temperature ratio ($\frac{T_w-T_0}{T_0}$)
φ axial angle, degree
μ viscosity, kg/(m s)
Θ nondimensional temperature ($\frac{T_w-T_0}{T_b-T_w}$)
ρ density of fluid, kg/m^3
σ Stefan–Boltzmann constant (5.6697×10^{-8}), $W/m^2 K^4$
σ_a absorption coefficient
σ_s scattering coefficient
τ optical thickness
τ_w wall shear stress, N/m^2
ω radiation solid angle, degree
Ω phase function

Subscripts
0 inlet conditions
2nd secondary flow
b bulk quantity
c convection
r radiation
t total (convection + radiation)
w wall condition

In a survey of the open literature on combined convective and radiation transfer in flow in pipe, it was found that most studies had been conducted for the straight pipes and curved pipe without pitch, such as those by Kamiuto and Kanemaru [17], Kim and Baek [18], Franca and Goldstein [19], Ramamurthy et al. [20], Chiou [21], Yang [22], Huang and Lin [23], Bestman [24], Yang and Ebadian [25], and Lin and Ebadian [26]. One of the principal features of the fluid flows in a helical pipe is the occurrence of a secondary flow in planes normal to the main flow, which causes the momentum and energy transport in the curved pipe to be substantially different from that of the flow in a straight pipe and dramatically increases the difficulty of theoretical analysis of the physical problem in a helical pipe.

This paper reports the performance of a fully elliptic numerical computation to study heat transfer of the combined convection and thermal radiation in laminar flow in a helical pipe with finite pitch. A control-volume finite difference method (CVFDM) was used to solve the governing equations, and an O-type structure grid was adapted to discretize the entire computation domain. To capture the physics, fully elliptic laminar flow governing equations coupled with a P-1 radiation model are employed in the numerical simulation. The effects of thermal radiation on flow and thermal fields and profiles with and without thermal radiation are discussed. The effects of Richardson number, pitch, and ratio of temperature on the developments of friction factors and Nusselt numbers with and without thermal radiation are presented and highlighted.

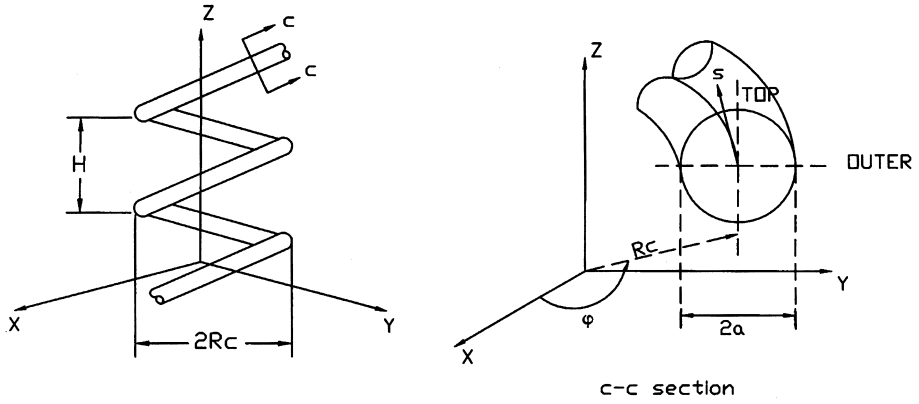

Fig. 1. Schematic geometry and coordinates of the helical pipe.

2. Mathematical formulation

2.1. Governing equations

The geometry considered and the system of coordinates are depicted in Fig. 1. The circular pipe has a diameter of $2a$ and is coiled at a radius of R_c, while the distance between two turns (the pitch) is represented by H. In this experiment, the Cartesian coordinate system (x, y, z) is used to represent a helical pipe in numerical simulation.

At the inlet ($\varphi = 0^\circ$), fluid at temperature T_0 enters the helical pipe at a speed of U_0. The wall of the pipe is heated under constant temperature T_w. Laminar flow and heat transfer develop simultaneously downstream in the helical pipe. The flow is considered to be steady, and constant thermal properties are assumed except for the density in the body force term that is modeled by ideal gas assumption. The fully elliptic differential equations governing the three-dimensional laminar flow in the helical pipe could be written in tensor form in the master Cartesian coordinate system as

State:

$$p = \rho RT \tag{1}$$

Mass:

$$\frac{\partial u_i}{\partial x_i} = 0 \tag{2}$$

Momentum:

$$\frac{\partial}{\partial x_j}\left[\mu\left(\frac{\partial u_i}{\partial x_j} + \frac{\partial u_j}{\partial x_i}\right) - \rho u_j u_i - \delta_{ij} p\right] + \rho g_i = 0 \tag{3}$$

Energy:

$$\frac{\partial}{\partial x_j}\left(k\frac{\partial T}{\partial x_j} - \rho u_j C_p T\right) + \mu\Phi_v + \nabla q_r = 0 \tag{4}$$

where q_r is the radiative heat flux to the fluid element, $\mu\Phi_v$ represents the viscous heating term in the energy equation, and Φ_v is defined as

$$\Phi_v = \frac{\partial u_i}{\partial x_j}\left(\frac{\partial u_i}{\partial x_j} + \frac{\partial u_j}{\partial x_i} - \frac{2}{3}\mu\frac{\partial u_i}{\partial u_j}\delta_{ij}\right) \tag{5}$$

2.2. Radiation model

The working fluid is assumed to be a gray, absorbing, emitting, and isotropically scattering medium. The radiative transfer equation governing the radiation intensity is given by

$$\frac{dI(x,\omega)}{dx} + (\sigma_a + \sigma_s)I(x,\omega) = \sigma_a\frac{\sigma T^4}{\pi} + \frac{\sigma_s}{4\pi}\int_0^{4\pi} I(x,\omega)\Omega\, d\omega \tag{6}$$

where the radiation intensity, I, depends on position (x) and solid angle (ω). σ_a is the absorption coefficient; σ_s is the scattering coefficient; σ is the Stefan–Boltzmann constant; and, Ω, the phase function. The optical thickness is defined as

$$\tau = (\sigma_a + \sigma_s)x \tag{7}$$

The P-1 approximation radiation model, described by Cheng [27] and Siegel and Howell [28], is employed in the present radiative heat transfer simulation. Previous studies indicate that P-1 approximation is more accurate in the optically thick rather than the optically thin limit. However, since the focus of this study concentrates the interaction of convection and radiation in absorbing–emitting media which is highly absorbing, the inaccuracy of the method of the P-1 approximation in the optically thin limit may not be a serious limitation [28]. The radiation heat flux, q_r, is determined

by the following equation:

$$\nabla q_r = \sigma_a G - 4\sigma_a \sigma T^4 \tag{8}$$

where G is the incident radiation. With C representing the linear-anisotropic phase function coefficient, the transport equation for G is written as

$$\nabla(B\nabla G) - \sigma_a G + 4\sigma_a \sigma T^4 = 0 \tag{9}$$

$$B = \frac{1}{3(\sigma_a + \sigma_s) - C\sigma_s} \tag{10}$$

2.3. Boundary conditions

Non-slip boundary condition, $u_i = 0$, and constant temperature, T_w, are imposed on the wall. The Marshak boundary condition is used to determine the radiation heat flux at the wall [28]. The net radiation heat flux at the wall, $q_{r,w}$, is obtained by the following equation:

$$q_{r,w} = \frac{\varepsilon_w}{2(2-\varepsilon_w)}\left(4\sigma T_w^4 - G_w\right) \tag{11}$$

where G_w is the incident radiation at wall; ε_w is emissivity of wall. In this study, the emissivity of the wall (ε_w) is set to 1.0 (i.e., black body absorption).

At the inlet, the following uniform profiles for all the dependent variables are employed for simplicity:

$$u_n = U_0, \qquad T = T_0 \tag{12}$$

where u_n is normal velocity perpendicular to the inlet plane. The net radiation heat flux at the inlet is computed in the same manner as at the wall and is also set to be black body absorption. According to the entry length data on coiled pipes given by Austin and Seader [29], the computation domain ($0^\circ \le \varphi \le 355^\circ$) used in this study can ensure the outflow condition (i.e., fully developed flow and thermal assumed) can be satisfied at the exit plane of the helical pipe. Therefore, at the outlet, the diffusion flux for all variables in the exit direction is set to zero:

$$\frac{\partial}{\partial n}(u_i, p, T) = 0 \tag{13}$$

where n is used to represent the normal coordinate direction perpendicular to the outlet plane. The net radiation heat flux at outlet is computed in the same manner at wall. Since the fully developed flow and thermal can be satisfied at outlet, the black body absorption can be assumed at outlet (i.e., the radiation coming from downstream of outlet does not affect the upstream thermal field).

2.4. Parameter definitions

To represent the results and characterize the combined heat transfer in helical pipes, the following nondimensional variables and parameters are defined as

$$Re = \frac{\rho u_0 d_h}{\mu}, \quad \delta = \frac{a}{R_c}, \quad \lambda = \frac{H}{2\pi R_c}$$

$$Gr = \frac{\rho^2 g\beta d_h^3}{\mu^2}(T_w - T_0), \quad f_\theta = \frac{\tau_w}{\frac{1}{2}\rho U_0^2},$$

$$f_m = \frac{1}{2\pi}\int_0^{2\pi} f_\theta \, d\theta, \quad Nu_\theta = \frac{q_w d_h}{k(T_w - T_b)},$$

$$Nu_m = \frac{1}{2\pi}\int_0^{2\pi} Nu_\theta \, d\theta, \quad T_b = \frac{1}{\bar{u}_s A}\int_0^A u_s T \, dA,$$

$$\Theta = \frac{T - T_w}{T_b - T_w}, \quad U_s = \frac{u_s}{U_0} \tag{14}$$

where δ is the curvature ratio; λ, nondimensional pitch; f_θ and Nu_θ, local friction factor and Nusselt number along the circumference of the pipe, respectively; and f_m and Nu_m, the circumference average friction factor and Nusselt number on one cross-section of the pipe, respectively. The term Θ represents nondimensional temperature, while U_s denotes nondimensional axial velocity on one cross-section of the pipe.

Further, when the thermal radiation is considered, the local total Nusselt number along the circumference of the helical pipe, Nu_θ, is composed of two parts (i.e., the local convective Nusselt number, $Nu_{\theta,c}$, and the local radiative Nusselt number, $Nu_{\theta,r}$)

$$Nu_\theta = Nu_{\theta,c} + Nu_{\theta,r} = \frac{q_{w,c} d_h}{k(T_w - T_b)} + \frac{q_{w,r} d_h}{k(T_w - T_b)} \tag{15}$$

where $q_{w,c}$ and $q_{w,r}$ are convective heat flux and radiative heat flux, respectively, on the wall of the helical pipe. The definition of the average Nusselt number is similar to the expression for the local Nusselt number

$$Nu_m = Nu_{m,c} + Nu_{m,r} \tag{16}$$

3. Numerical computation

3.1. Numerical method

The governing equations for combined laminar convection and thermal radiation heat transfer in the heli-

Table 1
Grid independent test ($Re = 1000$, $\delta = 0.05$, $\lambda = 0.25$, air)

Grids ($I \times J \times K$)	46×22×120	46×22×180	46×22×240	32×16×120	32×16×180	32×16×240	32×22×120	32×22×180
Total	121,440	182,160	242,880	61,440	92,160	122,880	84,880	126,720
V_{max}	1.008	1.019	1.014	0.989	0.992	0.996	0.999	1.003
$f_{m,\,max}$	0.047	0.039	0.038	0.043	0.039	0.038	0.047	0.039

cal pipe are solved in the master Cartesian coordinate system with a control-volume finite difference method (CVFDM) similar to that introduced by Patankar [30]. An O-type structure nonuniform grid system, shown in Fig. 2, has been used to discretize the computation domain. Fluent program [31,32] is used as a numerical solver for the present three-dimensional simulation. A non-staggered grid storage scheme is adapted to define the discrete control volumes. In this scheme, the same control volume is employed for integration of all conservation equations, and all variables are stored at the control volume cell center. The numerical scheme used in this study is a power-law differencing scheme. The final discrete algebraic equation for any variable ϕ at point P could be written as

$$A_P\phi_P = \sum_{NB} A_{NB}\phi_{NB} + S_\phi \tag{17}$$

where the subscript NB denotes neighbor value. The coefficients A_P and A_{NB}, contain convection and diffusion coefficients. S_ϕ is the source of ϕ in the control volume surrounding point P. The SIMPLE algorithm [33] is used to resolve the coupling between velocity and pressure. The algebraic equations are solved iteratively using an additive-correction multigrid method [34] with a Gauss–Seidel relaxation procedure. To accelerate convergence, the under-relaxation technique is applied to all dependent variables. In the present study, the under-relaxation factor for the pressure, p, is 0.3; that for temperature, T, is 0.9; that for the velocity component in the i-direction, u_i, is 0.5; and that for radiation intensity, I, is 0.8, and that for body force is 0.8.

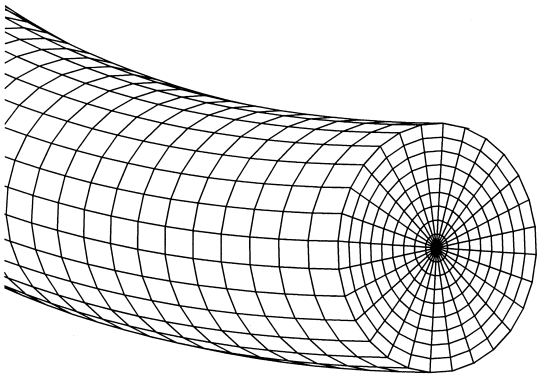

Fig. 2. Structured grid of the helical pipe.

3.2. Grid system

An O-type structured nonuniform grid system (Fig. 2) is adapted in this experiment. Two blocks are applied to form the entire computation domain. Compared with other structure grids in open literature, this O-type grid offers more control, with the grid spacing near the wall of pipe in cylindrical geometry, as well as lower skewness, which is better for modeling gradients. For this O-type grid, the centerline of the helical pipe is the singularity axis because multiple grid lines meet at a single point in three-dimensional simulations. To delete the singularity, the values at the centers of the cells surrounding a point on the axis are averaged and then assigned to each of the boundary cells bordering the axis in the circumference direction. The numerical solutions indicate this method is reasonable.

A grid refinement study is conducted to determine an adequate grid distribution. Table 1 presents a comparison of the predicted results at different grid distributions (circumference, radial, and axial) and the total grid numbers. The term V_{max} is the maximum value of magnitude of dimensional velocity, $V = \sqrt{u_1^2 + u_2^2 + u_3^2}$, and $f_{m,\,max}$ is the maximum value of f_m in the entire computation domain. This table indicates the grid distribution and total number have signature influence for numerical solution. The $46 \times 22 \times 180$ grid arrangement could ensure a satisfactory solution for fluid flow in the helical pipe. Thus, the present computations are based on this grid distribution. All the computations are carried out on a SGI Original 2000 at Florida International University's Hemispheric Center for Environmental Technology (FIU-HCET).

3.3. Convergence criterion

The numerical computation is considered converged when the residual summed over all the computational nodes at nth iteration, R_ϕ^n, satisfies the following cri-

terion:

$$\frac{R_\phi^n}{R_\phi^m} \leq 10^{-5} \tag{18}$$

where R_ϕ^m denotes the maximum residual value of ϕ variable after m iterations. ϕ applied for p, u_i, T, and I. For the computation of the combined convection and radiation heat transfer in helical pipe, the iteration number is almost two to three times higher than that required for the computation of pure convection in helical pipe.

4. Results and discussion

The following numerical results were obtained based on parameters of $\delta = 0.05$, $Pr = 0.7$, $Gr = 4 \times 10^4$, and $T_0 = 293$ K. For the cases of pure convection heat transfer, $\tau = 0.0$, for the cases of combined convection and thermal radiation heat transfer, $\tau = 1.0$. Validation of the mathematical model and numerical method described above were performed by Lin et al. [26] and Fluent Inc. [31] and would not be repeated in this study.

4.1. Development of flow fields

The numerical results of this study have shown that both velocity and temperature fields on one cross-section of helical pipe with thermal radiation considered are almost the same as those without thermal radiation under the present investigated conditions. Typical developments of axial velocity, secondary velocity, and temperature fields for pure convection ($\tau = 0.0$) are shown in Fig. 3, under the condition of $\delta = 0.05$, $\lambda = 1.0$, $Re^2/Gr = 10$, and $\Delta T = 0.6$, which mean that the inlet temperature is 293 K and the wall temperature is 468.8 K. It is shown that with the increase of φ, the secondary velocity is enhanced, and the high axial velocity and temperature zones shift to the outer side because of centrifugal force.

The axial velocity profiles are shown in Fig. 4. It shows that when φ is small, the velocity is almost symmetrical to center point on both horizontal and vertical centerlines. This result agrees with the axial velocity field. With the increase of φ, the axial velocity becomes asymmetrical. In the horizontal centerline, the maximum velocity shifts to the outside of the pipe because of the unbalanced centrifugal force on the main flow. In the vertical centerline, the velocity becomes a little asymmetrical because of buoyancy. Comparing pure convection with combined convection and thermal radiation in axial velocity profiles, it is found that there is little difference between their velocity magnitudes on the developing region (below 4%), but in the fully developed region, the velocity magnitudes were almost the same.

The temperature profiles with and without thermal radiation are shown in Fig. 5. They are similar to the axial velocity profiles, but buoyancy has stronger effects in the temperature profiles than in axial velocity profiles. It could be said, under the present investigative conditions, the flow and temperature fields in the helical pipe are not sensitive to the thermal radiation when they are developed. The buoyancy has more effects in the temperature field than in the velocity field.

4.2. Development of local friction factor and Nusselt number

The developments of the local friction factor and Nusselt number with the increase of φ on the circumference of the helical pipe are shown in Fig. 6. The data were plotted from outermost point $\theta = 0^\circ$ to 360° in anti-clockwise direction along the circumference on one cross-section. Generally speaking, within the region near the inlet, the distribution of f_c (or Nu_θ) on the circumference is relatively smooth. As the flow proceeds downstream, the difference of f_c (or Nu_θ) between the maximum and minimum magnitude in the pipe increases. When the thermal radiation is active, there is a little difference for local friction factor with and without thermal radiation in the entrance region (below 5%), and near the outlet, they are almost the same. There is evident difference for the local Nusselt number magnitude with and without thermal radiation; the latter is higher than the former; the difference was about 30%. It could be said that when thermal radiation is activated, total heat transfer can be substantially enhanced.

4.3. Development of average friction and Nusselt number

4.3.1. Effect of Richardson number

The effects of Richardson number on the developments of the circumference average friction factor and Nusselt number are shown on Fig. 7 with $\lambda = 1.0$, $\Delta T = 0.2$. The whole process of the developments of f_m (or Nu_m) could be divided into three stages characterized by a substantial difference nature. These are summarized below:

1. the early developing stage ($\varphi < 15^\circ$), where f_m (or Nu_m) dropped sharply at the increase of φ due to the rapid development of the flow (or thermal) boundary layer;
2. the oscillatory developing stage ($15^\circ < \varphi < 180^\circ$), where obvious oscillation of f_m (or Nu_m) appeared with the increase of φ;
3. the later developing stage ($\varphi > 180^\circ$), when f_m (or

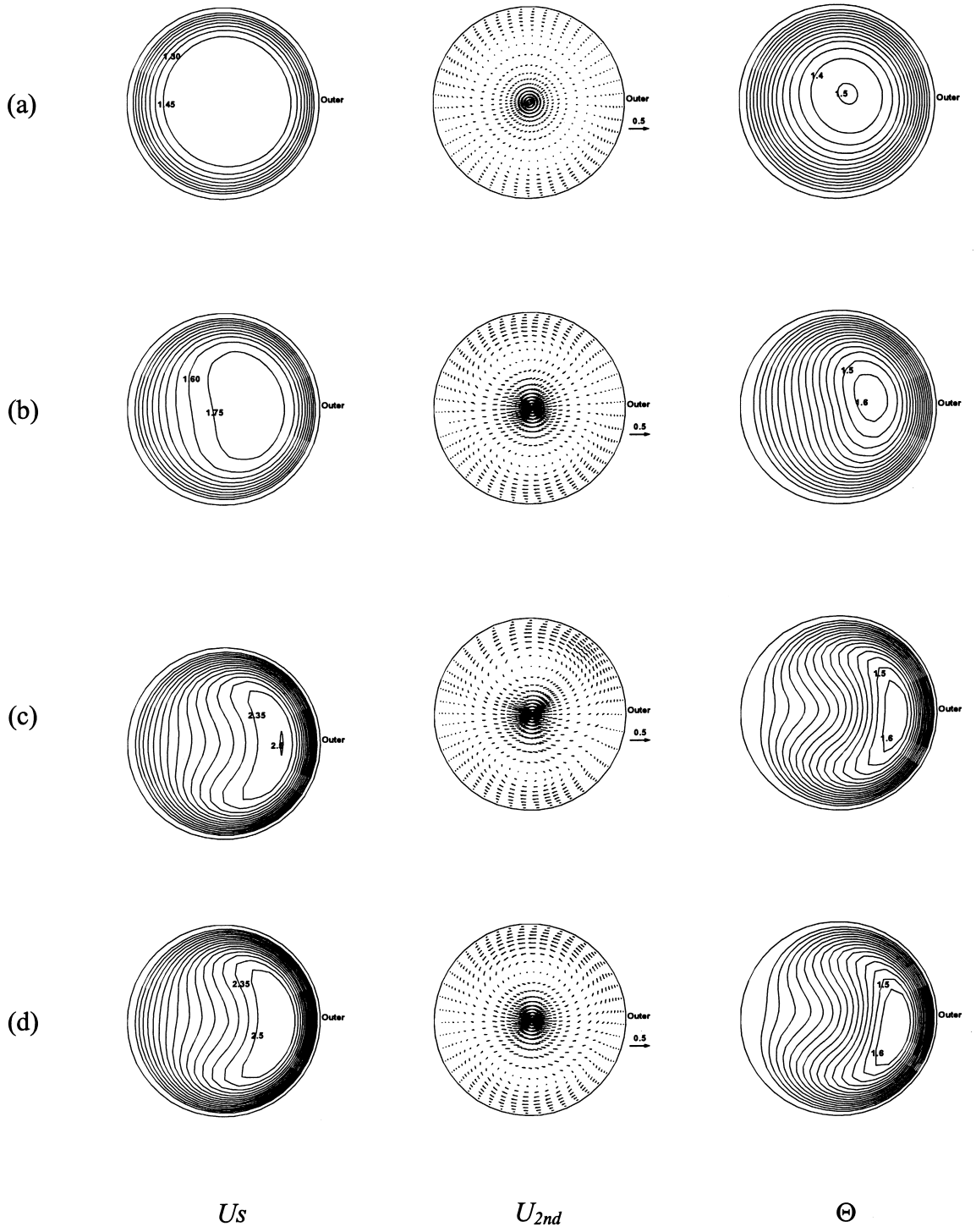

Fig. 3. Developments of velocity and temperature field, $Re^2/Gr = 10$, $\lambda = 1.0$, $\Delta T = 0.6$, $\tau = 0.0$. (a) $\varphi = 15^\circ$, (b) $\varphi = 30^\circ$, (c) $\varphi = 120^\circ$, (d) $\varphi = 340^\circ$.

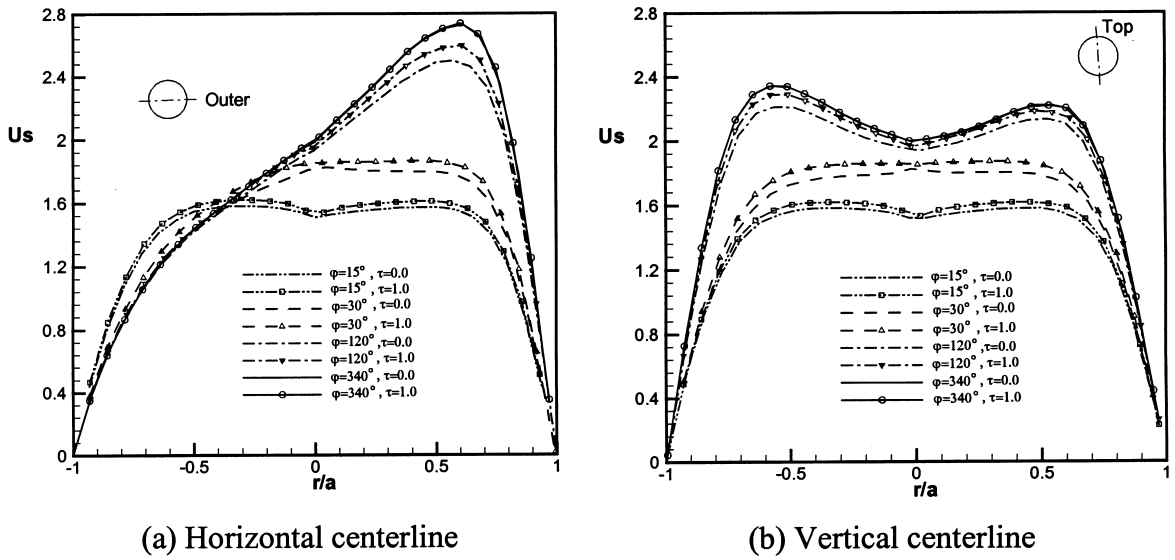

Fig. 4. Developments of axial velocity profile with and without thermal radiation in horizontal centerline (a) and vertical centerline (b), $Re^2/Gr = 10$, $\lambda = 1.0$, $\Delta T = 0.6$.

Nu_m) varied smoothly with the increase of φ until the fully developed flow (or heat transfer) was established.

Under the computational conditions used in Fig. 7, the effect of Richardson number was to reduce the magnitude of f_m and, in contrast, increase the magnitude of Nu_m. As shown in the figure, for pure convection and combined convection and radiation, both of the average friction factors have almost the same value. Both convective Nusselt numbers have almost the same value too, even though one is pure convection Nu_m and the other is part convection in total Nusselt number with thermal radiation, $Nu_{m,c}$. The total Nu_m with thermal radiation is much higher than that in pure

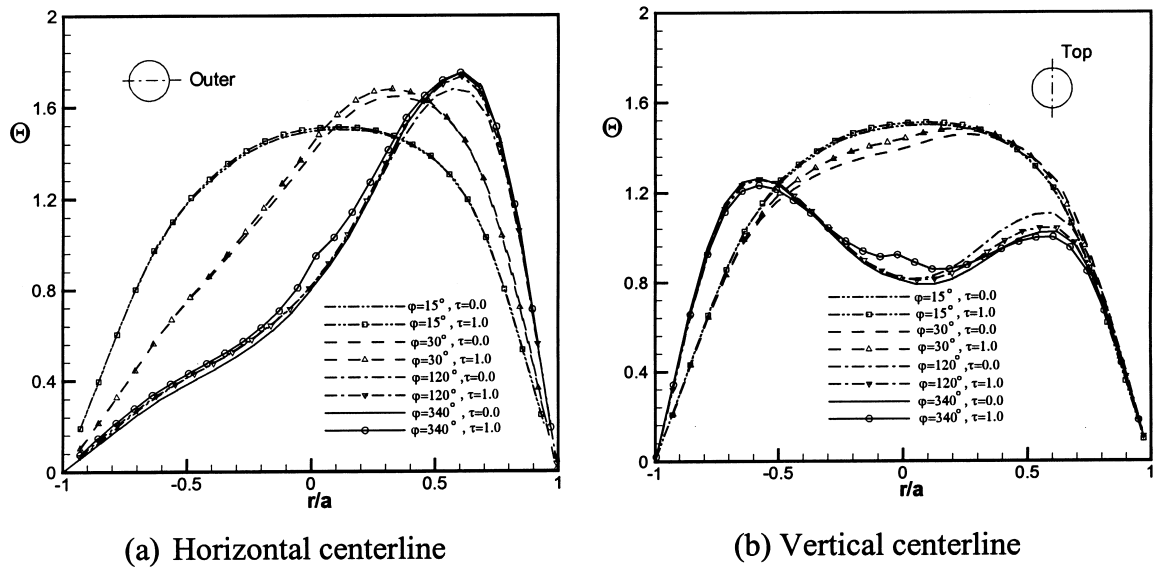

Fig. 5. Developments of temperature profile with and without thermal radiation in horizontal centerline (a) and vertical centerline (b), $Re^2/Gr = 10$, $\lambda = 1.0$, $\Delta T = 0.6$.

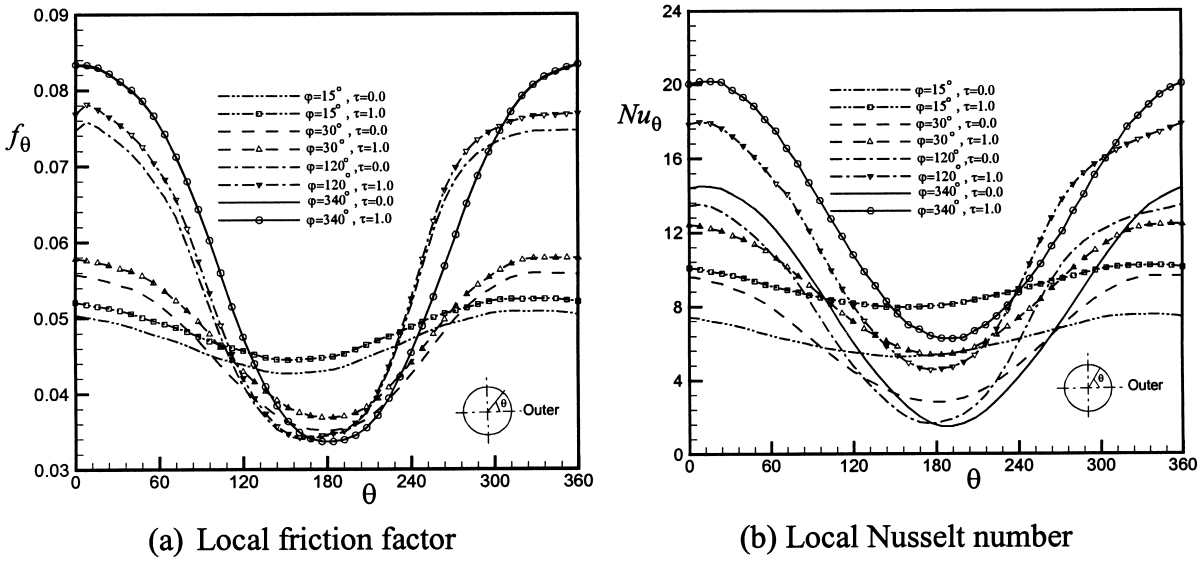

Fig. 6. Developments of local friction factor (a) and local Nusselt number (b) on the circumference of helical pipe with and without thermal radiation, $Re^2/Gr = 10$, $\lambda = 1.0$, $\Delta T = 0.6$.

convection (the difference of magnitude exceeded 30%). In these cases, since the temperature ratio is relatively small ($\Delta T = 0.2$), so the convective heat transfers with and without thermal radiation are almost the same.

4.3.2. Effects of pitch

Fig. 8 demonstrates the effect of pitch, λ on the development of average friction factor and Nusselt number with $Re^2/Gr = 10$, $\Delta T = 0.2$. The pitch exerts a similar influence on the developing f_m as it does on

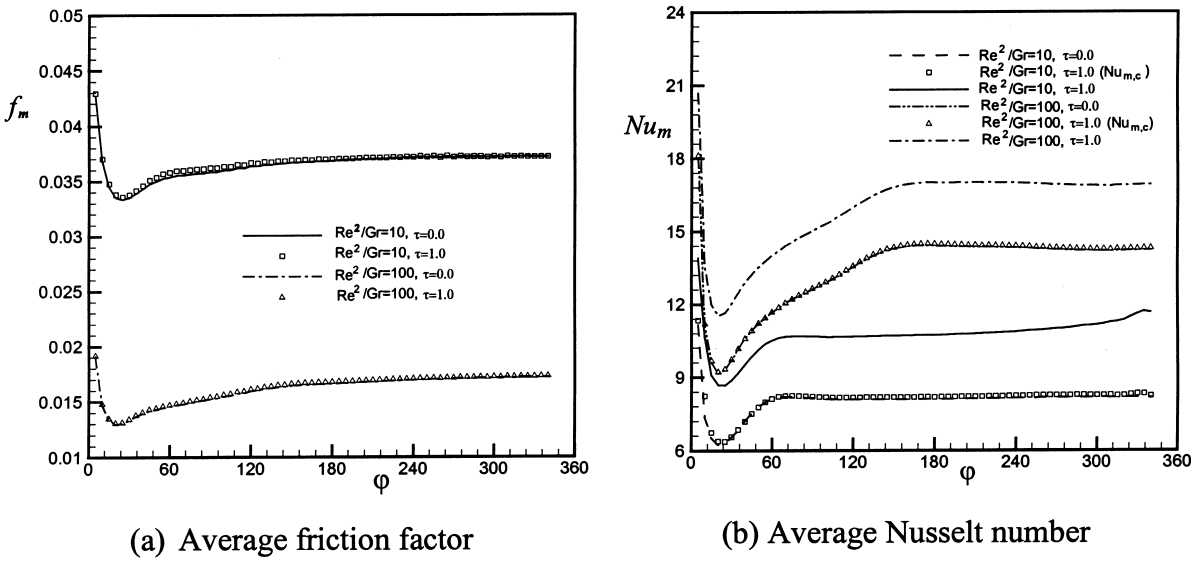

Fig. 7. Effects of Richardson number (Re^2/Gr) on the development of average friction factor (a) and Nusselt number (b) with and without thermal radiation, $\lambda = 1.0$, $\Delta T = 0.2$.

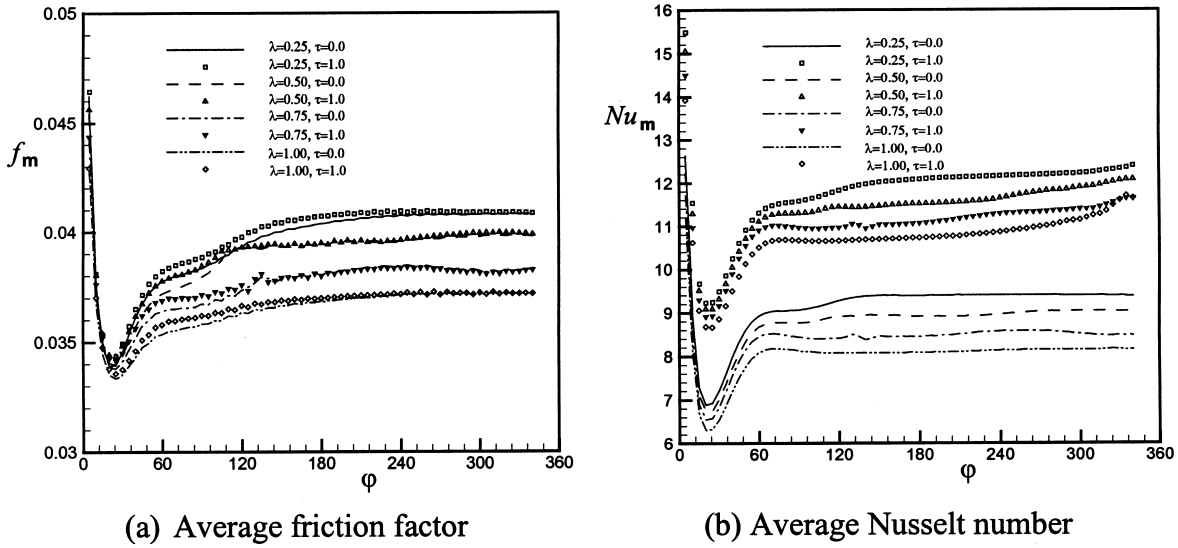

Fig. 8. Effects of pitch on the development of average friction factor (a) and Nusselt number (b) with and without thermal radiation, $Re^2/Gr = 10$, $\Delta T = 0.2$.

the developing Nu_m, whether with or without thermal radiation. In the course of flow and heat transfer developments of the helical pipe, the effect of pitch, λ, is to reduce the magnitude of f_m and Nu_m at different axial locations. In Fig. 7, with increase of λ, the developing region of the combined convective and thermal radiation heat transfer is increased and becomes oscillated. Similarly, with the effects of Richardson number, both the friction factors with and without thermal radiation have almost the same value when the flow is fully developed.

4.3.3. Effects of temperature ratio

The temperature ratio is an important factor in radiation heat transfer. In this study, the Gr is set constant when the temperature ratio is varied. The physics properties are dependent on fixed Gr, which means that the physics properties in different cases are different. Under examined conditions, the effects of temperature ratio, ΔT, on the developments of f_m and Nu_m are shown in Fig. 9 with $\lambda = 1.0$, $Re^2/Gr = 10$. In Fig. 9, with the increase of ΔT, the magnitude of f_m and Nu_m ($\tau = 1.0$) are increased, and in contrast, the pure convection Nu_m ($\tau = 0.0$) almost remains the same when they are developed. The pure convection heat transfer is mainly dependent on Gr under these conditions, so when Gr is set constant, the pure convection heat transfer is also the same. With the increase of ΔT, the difference between friction factors with and without thermal radiation is increased in the developing region, and the friction factor with thermal radiation could reach the fully developed stage earlier than that without thermal radiation. With the increase of ΔT, the velocity gradient with thermal radiation in the pipe wall varies rapidly, so the friction factor rapidly reaches fully developed due to the increasing effect of buoyancy. With the increase of ΔT, the developing region of heat transfer with thermal radiation is increased, and when $\Delta T > 0.6$, this computation domain ($\varphi = 0°$–$355°$) does not satisfy the request of fully developed. The radiation heat transfer could not reach fully developed in this computation domain. Further research to determine the reasonable limit for the developing region when thermal radiation is activated is requested.

5. Conclusions

The combined convection and thermal radiation heat transfer in three-dimensional laminar flow through a helical pipe with finite pitch has been simulated with the CVFDM method. Under the investigated conditions and parameters range, the following conclusions could be drawn:

1. There is no evident influence of thermal radiation on axial velocity, second velocity, and temperature fields when only the radiation participating medium is considered. The difference of magnitude may be ignored. The buoyancy has more effects in temperature field than it has in velocity field.
2. The total heat transfer in helical pipe could be substantially enhanced when thermal radiation is taken into account. The friction factor is not sensitive to

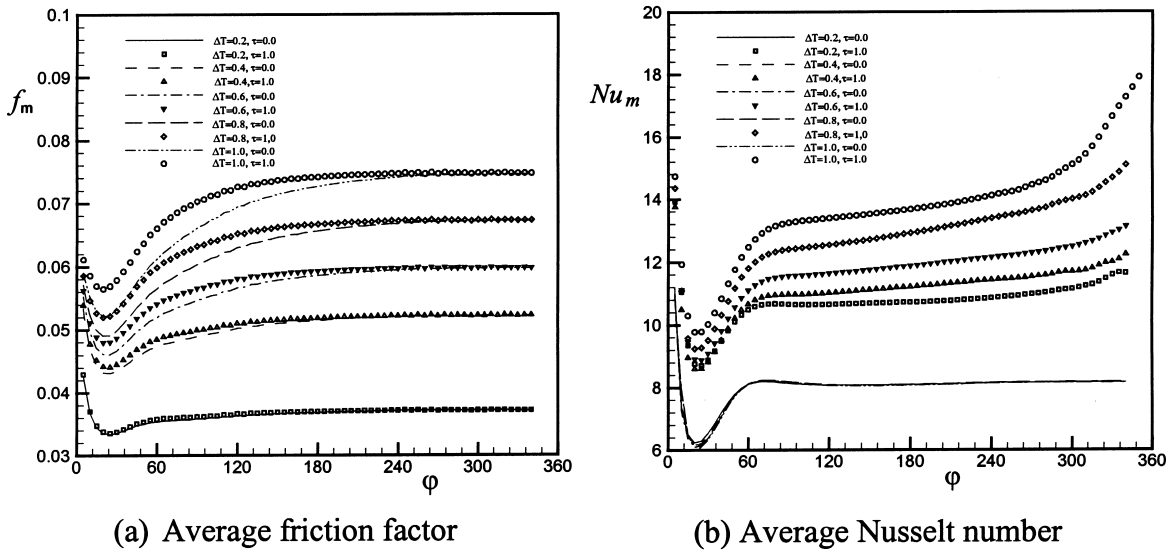

Fig. 9. Effect of temperature ratio on the development of average friction factor (a) and Nusselt number (b) with and without thermal radiation, $Re^2/Gr = 10$, $\lambda = 1.0$.

thermal radiation, especially in the fully developed region.

3. With the decrease of Re^2/Gr, the combined heat transfer capability in helical pipe increases, and the magnitude of average friction factor is decreased. The effect of pitch is to decrease the magnitude of average friction factor and Nusselt number. With increasing pitch, the developing region also increases.
4. Under the computed conditions in this study, the temperature ratio has significant influence on the total heat transfer when thermal radiation is active and has little influence on pure convective heat transfer. The increase of temperature ratio not only increases the heat transfer with radiation, it also increases the developing region.

Acknowledgements

The authors gratefully acknowledge the financial support of the National Science Foundation (NSF) under Grant No. CTS-9017732.

References

[1] S.A. Berger, L. Talbot, L.S. Yao, Flow in curved pipes, Annual Review of Fluid Mechanics 15 (1983) 461–512.
[2] R.K. Shah, S.D. Joshi, Convective heat transfer in curved ducts, in: S. Kakac, R.K. Shah, W. Aung (Eds.), Handbook of Single-Phase Convective Heat Transfer, Wiley, New York, 1987 (Chapter 5).
[3] D.J. Goering, J.A.C. Humphrey, R. Greif, Dual influence of curvature and buoyancy in fully developed tube flows, International Journal of Heat and Mass Transfer 40 (1997) 2187–2199.
[4] C.X. Lin, P. Zhang, M.A. Ebadian, Laminar forced convection in the entrance region of helical pipes, International Journal of Heat and Mass Transfer 40 (1997) 3293–3304.
[5] C.J. Bolinder, B. Sunden, Numerical prediction of laminar flow and forced convective heat transfer in a helical square duct with a finite pitch, International Journal of Heat and Mass Transfer 39 (1996) 3101–3115.
[6] J.J.M. Sillekens, Laminar mixed convection in ducts, PhD thesis, Technische Universiteit Eindhoven, Dutch, 1995.
[7] V.G. Yang, Z.F. Dong, M.A. Ebadian, Laminar forced convection in a helicoidal pipe with finite pitch, International Journal of Heat and Mass Transfer 38 (1995) 853–862.
[8] J.H. Chung, J.M. Hyun, Heat transfer from a fully-developed pulsating flow in a curved pipe, International Journal of Heat and Mass Transfer 37 (1994) 43–52.
[9] R. Yang, S.F. Chang, Combined free and forced convection for developed flow in curved pipes with finite curvature ratio, International Journal of Heat and Fluid Flow 15 (1994) 470–476.
[10] B.K. Rao, Turbulent heat transfer to power-law fluids in helical passages, International Journal of Heat and Fluid Flow 15 (1994) 142–148.
[11] S. Liu, J.H. Masliyah, Developing convective heat trans-

fer in helical pipes with finite pitch, International Journal of Heat and Fluid Flow 15 (1994) 66–74.
[12] M.D. Su, R. Friedrich, Numerical simulation of fully developed flow in a curved duct of rectangular cross-section, International Journal of Heat and Mass Transfer 37 (1994) 1257–1268.
[13] R.M. Eason, Y. Bayazitoglu, A. Meade, Enhancement of heat transfer in square helical ducts, International Journal of Heat and Mass Transfer 37 (1994) 2077–2087.
[14] D.D. Joye, A.G. Hakun, C.D. Joye, Heat transfer in helical, curved rectangular channels; comparison of type I and type II systems, International Journal of Heat and Mass Transfer 36 (1993) 3541–3546.
[15] N. Acharya, M. Sen, H.C. Chang, Thermal entrance length and Nusselt numbers in coiled tubes, International Journal of Heat and Mass Transfer 37 (1993) 336–340.
[16] J. Vilemas, P. Poskas, V. Simonis, V. Sukys, Heat transfer and hydraulic drag in helical channels in gas flow, International Journal of Heat and Mass Transfer 36 (1993) 1693–1700.
[17] K. Kamiuto, K. Kanemaru, Approximate method for combined forced-convection and radiation heat transfer in absorbing and emitting gases flowing in a black, plane-parallel duct, International Journal of Heat and Mass Transfer 39 (1996) 2191–2193.
[18] T.Y. Kim, S.W. Baek, Thermal development of radiatively active pipe flow with nonaxisymmetric circumferential convective heat loss, International Journal of Heat and Mass Transfer 39 (1996) 2969–2976.
[19] F.H.R Franca, L. Goldstein, Jr., Heat transfer combining convection, conduction and radiation in the flow of heated air through an insulated tube, The American Society of Mechanical Engineers, Paper no. 95-WA/HT-48, 1995.
[20] H. Ramamurthy, S. Ramadhyani, R. Viskanta, Two-dimensional axisymmetric model for combusting, reacting and radiating flows in radiant tubes, Journal of the Institute of Energy 67 (1994) 90–100.
[21] J.S. Chiou, Combined radiation-convection heat transfer in a pipe, Journal of Thermophysics and Heat Transfer 7 (1993) 178–180.
[22] L.K. Yang, Forced convection in a vertical pipe with combined buoyancy and radiation effects, International Communications in Heat and Mass Transfer 19 (1992) 249–262.
[23] J.M. Huang, J.D. Lin, Radiation and convection in circular pipe with uniform wall heat flux, Journal of Thermophysics and Heat Transfer 5 (1991) 502–507.
[24] A.R. Bestman, Radiative heat transfer to flow of a combustion mixture in a vertical pipe, International Journal of Energy Resources 15 (1991) 179–184.
[25] G. Yang, M.A. Ebadian, Thermal radiation and laminar forced convection in the entrance region of a pipe with axial conduction and radiation, International Journal of Heat and Fluid Flow 12 (1991) 202–209.
[26] C.X. Lin, M.A. Ebadian, Combined laminar forced convection and thermal radiation in a curved pipe, in: AIAA/ASME Joint Thermophysics and Heat Transfer Conference, vol. 1, ASME, New York, 1998.
[27] P. Cheng, Two-dimensional radiating gas flow by a moment method, AIAA Journal 2 (1964) 1662–1664.
[28] R. Seigel, J.R. Howell, Thermal Radiation Heat Transfer, Hemisphere, Washington, DC, 1992.
[29] L.R. Austin, J.D. Seader, Entry region for steady viscous flow in coiled circular pipes, AIChE J 20 (1974) 820–822.
[30] S.V. Patankar, Numerical Heat Transfer and Fluid Flow, Hemisphere, Washington, DC, 1980.
[31] Fluent Users Guide, version 4.4, Fluent Inc., Lebanon, NH, 1996.
[32] Geomesh Users Guide, release 3.0, Fluent Inc., Lebanon, NH, 1996.
[33] J.P. Van Doormaal, G.D. Raithby, Enhancements of the SIMPLE method for predicting incompressible flow problem, Numerical Heat Transfer 7 (1984) 147–158.
[34] B.R. Hutchinson, G.D. Raithby, A multigrid method based on the additive correction strategy, Numerical Heat Transfer 9 (1986) 511–537.